Compatibilization of biodegradable PGA/PBAT blends for enhancing mechanical and gas barrier properties

Paresh Kumar Samantaray [a], Christopher Ellingford [a], Stefano Farris [b], Tony McNally [a], Bowen Tan[c], Zhaoyang Sun[c], Yang Ji[c], Chaoying Wan[a]*

[a] International Institute for Nanocomposites Manufacturing (IINM), WMG, University of Warwick, CV4 7AL, U.K.

[b] Department of Food, Environmental and Nutritional Sciences, University of Milan, 20133, Milano, Italy

[c] PJIM Polymer Scientific Co., Ltd., Shanghai, 201102, China

ABSTRACT

Inappropriate disposal of single-use plastics alongside mismanagement of plastic wastes have been key drivers to plastics pollution and its replacement with biodegradable polymers can offer opportunities for circular plastics recycling. Poly(glycolic acid) (PGA) has the unique characteristics such as high degree of crystallinity, high thermal stability, high gas barrier properties and 100% compostability, however, PGA is mechanical brittle and moisture-sensitive, which has limited its applications in film packaging applications. In this study PGA was blended with poly (butylene adipate-co-terephthalate) (PBAT) in the presence of an epoxy-based compatibilizer (AX8900) via melt-extrusion to achieve flexible packaging films. The use of AX8900 not only promoted the ductility of 50/50 (w/w) PGA/PBAT blends but also enhanced the oxygen permeation and water vapour barrier performance of the blends. With addition of 20 wt. % AX8900, the strain at break improved from 10.7 % for 50/50 PGA/PBAT blend to ~150 % for 50/50/20 PGA/PBAT/AX8900 blends. While the oxygen permeance marginally reduced from 125(cm^3 mm) / (m^2 24h atm) for 50/50 PGA/PBAT to 116 (cm^3 mm) / (m^2 24h atm) for 50/50/20 PGA/PBAT/AX8900, water vapour barrier performance improvised by ~40 % and ~47 % respectively upon the addition of 10 wt. % and 20 wt. % AX8900 compared to 50/50 PGA/PBAT blend.

1. Introduction

Bioplastics are polymers that are bio-based, biodegradable, or both.[1] It implies that bioplastics have two aspects of sustainability, green educt and/or green product. While green educt implies the bioplastics generated from the feedstock or derived biologically, green product implies that the derivative products will be degradable and have a low impact on the environment.[2] Further, life-cycle

analyses of bioplastics indicate that they can reduce carbon dioxide (CO_2) emissions by 30-70% compared with conventional plastics.[3] Interestingly, in the recent market data report by Nova Institute, bioplastics are shown to represent ~ 1 % of the annual plastics production of 359 million tonnes.[3] With intriguing sophisticated applications and emerging biodegradable alternatives, the market for bioplastics is increasing at an astonishing rate. While globally, the current production capacity is estimated at around 2.11 million tonnes, it will increase and diversify up to 2.43 million tonnes by 2024.[3]

Poly (lactic acid) PLA is the most commonly used bioplastic.[4] Despite high mechanical properties, melt-processability, and transparency of PLA, its poor thermal stability, low gas barrier properties, and slower degradation rate limits its applications in food packaging. In this regard, its chemical analogue, poly (glycolic acid) PGA, exhibits higher mechanical strength, higher heat distortion temperature, and exceptional gas barrier properties due to its higher degree of crystallinity (~50 %). In addition, PGA has a faster degradation rate than PLA and is also 100% compostable under both industrial and home composting conditions.[4-5] However, the high degree of crystallinity of PGA leads to mechanical brittleness, which hinders its applications in flexible packaging.

Poly(butylene adipate-co-terephthalate) (PBAT) is an aliphatic-aromatic biodegradable polyester that has an exceptional extension at break.[6-7] It is often blended with other polymers such as PLA for enhancing ductility and toughness,[8-11] where a good compatibility between the polymer components is a prerequisite.[6] PGA being a structural analogue of PLA having similar solubility parameter (δ_{PGA}: 23.5 $MPa^{1/2}$, δ_{PLA}: 20.2 $MPa^{1/2}$), it also faces similar compatibility challenges when blended with PBAT. Reactive extrusion has been successfully applied in melt-processing of polymer blends with *in-situ* compatibilization. Using a free radical initiator dicumyl peroxide (DCP), *in-situ* compatibilization was realised during melt-blending of PLA and PBAT.[12] Due to the uncontrolled nature of this approach, products including branched and crosslinked PLA or PBAT, PLA-g-PBAT copolymers and PLA crosslinked with PBAT were all formed. Inclusion of 0.5 wt.% DCP, 80/20 PLA/PBAT blends showed greater compatibility through reduced PBAT domain size, yielding a strain at break of up to 300%, combined with increased toughness and tensile strength.

Utilising the carboxylic acid chain end groups in PLA and PBAT for reactive extrusion with chain extenders is an alternative approach for compatibilisation.[13] 2,2'-(1,3-phenylene)bis(2-oxazoline) and phthalic acid were used in tandem in an 80/20 PLA/PBAT blend demonstrated high strain (516%) and high strength. The increased interfacial adhesion between PLA and PBAT, as well as a decrease in the crystallinity of the blend was attributed to the mechanical performance obtained. Furthermore, transesterification of PLA/PBAT *via* 0.4 wt.% tetrabutyl titanate led to a 70/30 PLA/PBAT blend demonstrating high strength and strain properties through enhanced phase compatibility.[14]

Recently, Sarul et al. used cellulose nanocrystals (CNCs), to compatibilize PLA and PBAT based blends. Thermodynamically, CNCs had stronger affinity towards the PBAT phase however with higher CNC loadings (3 wt. % and 5 wt. %), the authors proposed the CNCs were located at the interface as well as in the PLA phase. This led to appreciable Young's modulus of PLA composite but low extension at break ~4 % for 5 wt. % CNC loading.[15] da Silva et al. used Cardolite®NC-514, a bio-based epoxy-cardanol pre-polymer (ECP) for compatibilizing PLA/PBAT blends. It was observed that the 1 and 3 wt. % ECP was an effective compatibilizer which showed significant improvement in elongation at break and a slight increment in tensile strength compared to non-compatibilized blends. Their results were superior compared to commercial Joncryl ADR 4300 (multi-epoxy functional chain extender by BASF) for the same concentration.[16] Abdelwahab et al. used glycidyl methacrylate monomer as a toughening agent for PLA and organosolv lignin based polymer blends. It was observed that by blending the epoxy-based agent (glycidyl methacrylate) to PLA itself, the elongation at break was enhanced from 3.3 % to 401 %.[17] This result suggests that epoxy-based compatibilizers may also work for compatibilizing PGA and PBAT blends.

Hence, in this work, we report a new strategy to compatibilize PGA and PBAT based co-continuous blends by reactive extrusion using a terpolymer of ethylene, methyl acrylate, and glycidyl methacrylate for improving extension at break while rendering good moisture and oxygen barrier performance. The blends were characterized using thermal characterization techniques, differential scanning calorimetry (DSC), thermogravimetric analysis (TGA) and moisture and oxygen barrier performance evaluated at 23°C and 65 % RH and, 23°C, 0 % and 50 % RH, respectively. The surface and cross-section electron micrographs revealed that these blends were effectively compatibilized and can be suitably used in flexible packaging films.

2. Materials and Methods

2.1. Materials

PGA was obtained from PJIM Polymer Scientific Co. Ltd. with a number av. molecular weight of 10^5 g/mol. PBAT used in the study was Ecoflex F BX 7011 by BASF with a number av. molecular weight of 1.42×10^5 g/mol. A ter-polymer of ethylene, methyl acrylate, and glycidyl methacrylate with 8% glycidyl methacrylate and 24% methyl acrylate with the trade name Lotader AX8900 (hereafter termed as AX8900) was kindly gifted by SK functional polymers. The number av. molecular weight of the polymer was 4.5×10^4 g/mol. The chemical structures and interactions of PGA, PBAT and AX8900 were shown in Scheme 1.

2.2. Blend preparation

For blending experiments, PGA/PBAT 50/50 (w/w) composition was optimized, and AX8900 was varied from 10-30% (w/w). (The blends throughout the manuscript were named PGA/PBAT/AX8900

50/50/10, 50/50/20, and 50/50/30, respectively.) Before extrusion, PGA and PBAT were dried in desiccant dryers overnight at 80 $^{\circ}$C. The extrusion was performed on Eurolab 16 (Thermo Fisher Scientific) twin-screw extruder with an L/D ratio of 40:1. Zone 2 was set to 100 $^{\circ}$C, while zone 3 to 220 $^{\circ}$C, zones 4 through 7 to 240 $^{\circ}$C, 8 and 9 were set to 230 $^{\circ}$C and the final zone, 10 was set to 220 $^{\circ}$C. The feed was set at 6 %, and a screw speed of 120 rpm was used for all experiments.

2.3. *Blend characterization*

Fourier-Transform Infrared spectroscopy (FTIR) was performed on a Bruker TENSOR 27 in the spectral range 4000 to 650 cm^{-1} at a resolution of 4 cm^{-1} with 64 scans. Differential scanning calorimetry (DSC) was carried out using a DSC 1 by Mettler Toledo. 5-8 mg of a polymer was placed within a DSC pan and then analyzed under a constant nitrogen flow rate of 50 mL/min. The experiments were performed using 10 K/min for both heating and cooling cycles. Thermogravimetric analysis (TGA) was performed on a Mettler Toledo instrument operating with a nitrogen flow rate of 50 mL/min and a heating rate of 10 K/min, heating from room temperature to 500 $^{\circ}$C. For mechanical testing, blends were pelletized and injection moulded as per ASTM D 638 standards using a Haake Minijet Pro piston injection moulding machine. The mechanical testing was performed on 300 kN Static Instron with a 10 kN fixture and a strain rate of 10 mm/min up to 110 % elongation and then at 25 mm/min until the sample broke. Scanning electron microscopy (SEM) was performed using a Zeiss Sigma. Oxygen transmission rate (OTR) and water vapour transmission rate (WVTR) were measured using a Totalperm permeabilimeter by Permtech, according to ASTM 3985 (OTR at 23°C and 0% RH), ASTM F1927 (OTR at 23 °C and 50% RH) and ASTM F1249 (WVTR at 23°C and 65% RH). To reset any influence arising from different film thicknesses, transmission rate values were converted to permeability coefficient – P′O$_2$ (cm^3 mm /m^2 24h atm) and P′WV (g mm /m^2 24h atm).

3. Results and Discussions

Figure 1 shows the normalized FTIR-ATR spectra of the blends in film form. Pristine PGA shows an ester stretching band at 1737 cm^{-1}, while PBAT shows the -C=O ester stretch at 1711 cm^{-1}. The -OH stretching at 3424 cm^{-1} was observed for PBAT in Figure 1(b). In PGA/PBAT 50/50, the PGA ester stretching peak shifts to 1733 cm^{-1} while the PBAT ester stretch shifts to 1720 cm^{-1}, attributed to a change in the polymer crystalline structure. The -OH stretching due to PBAT was also observed at 3514 cm^{-1}, see Figure 1(b). With the addition of 10 wt.% AX8900, the shift in ester and carbonyl groups is prominent at 1731 cm^{-1} and 1715 cm^{-1} but a change in PGA ester intensity was observed with respect to PBAT, indicating that some of the PGA ester groups were hydrogen bonding with the hydroxyl group of PBAT. In addition, the -OH stretching observed in the PGA/PBAT/AX8900 (50/50/10) blend broadened and shifted to a lower wavenumber, indicating further that the newly formed hydroxyl group of AX8900 interacted with esters along the PBAT and PGA chains. Similar observations were also seen in the blends containing 20 and 30 wt.% AX8900 blends, where the shift in the PGA ester and PBAT

ester are observed at 1731 and 1715 cm^{-1}, respectively for the 20 wt.% AX8900 blend; and 1731 and 1716 cm^{-1}, respectively, for the 30 wt.% AX8900 blend.

The free carboxylic acid end group in PBAT can react with the glycidyl end of AX8900 to form ester derivatives as per the mechanism proposed by Shechter et al.[18] It is important to note that sufficient glycidyl groups are required for this reaction, since AX8900 only contains 8 % of glycidyl moieties, we therefore selected a concentration > 10 % in our studies. The reaction schematic for the blends is proposed in scheme 1.
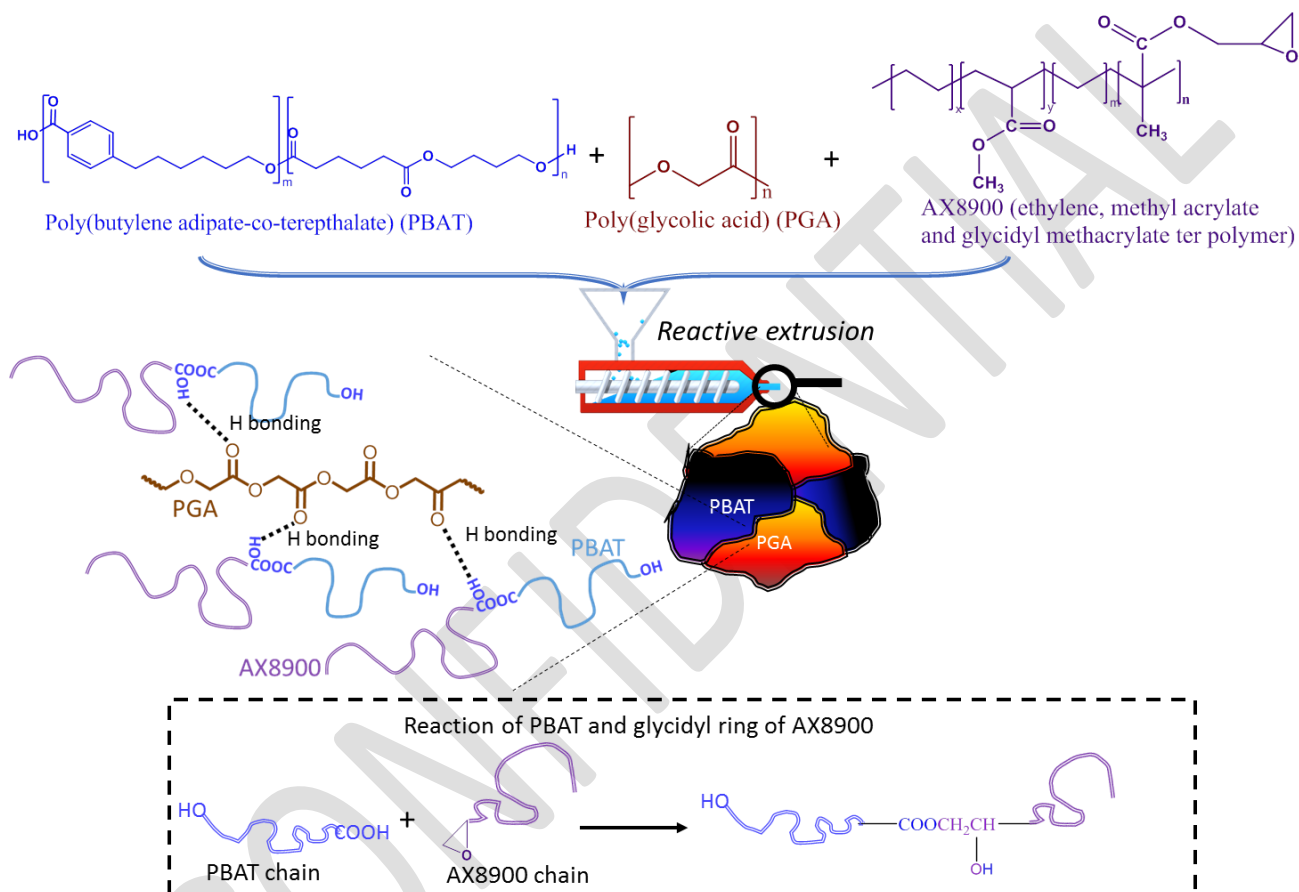
Scheme 1: Schematic representation of Compatibilization interaction between PGA, PBAT, and AX8900 after extrusion.
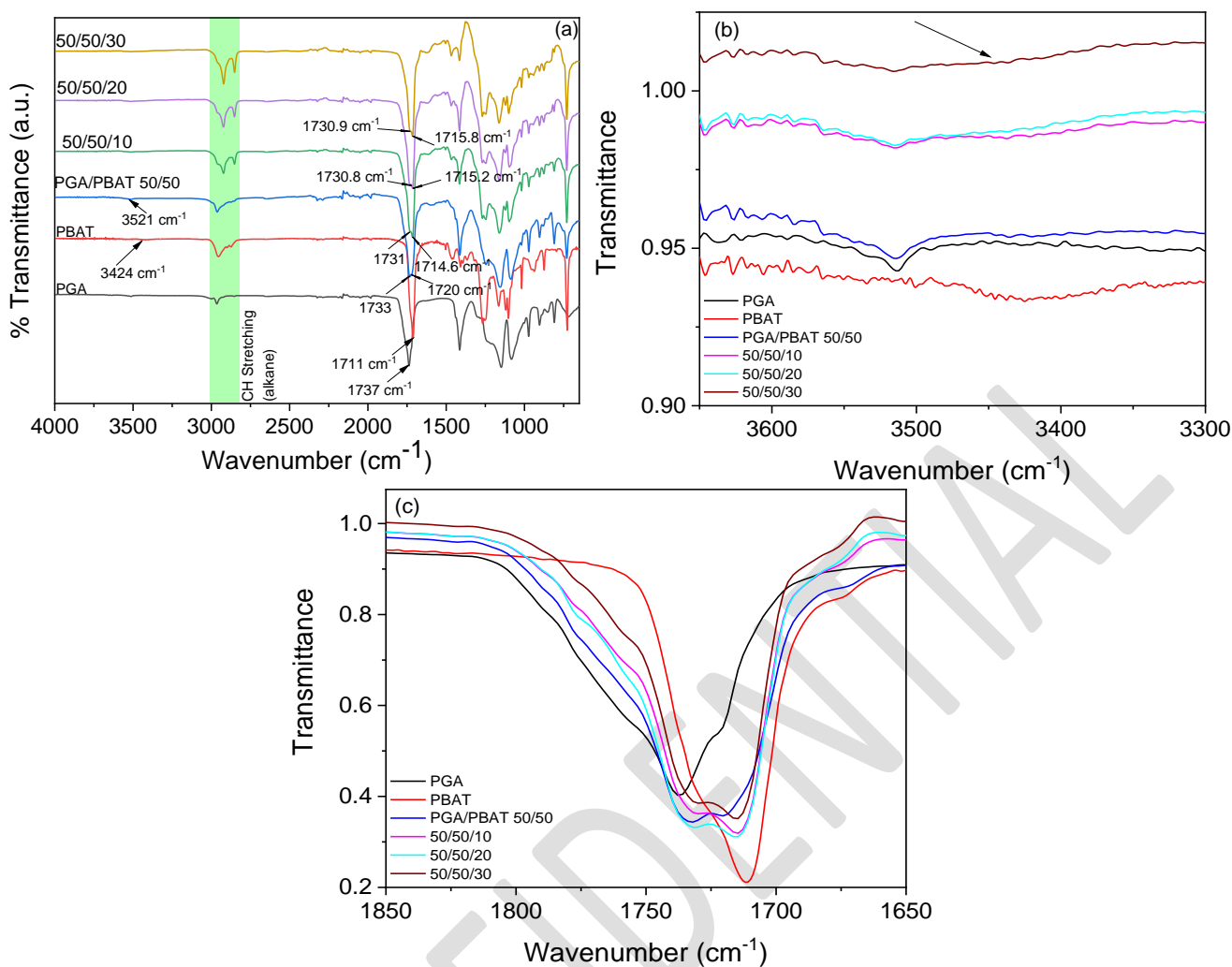
Figure 1: (a) FTIR of the polymers and blend compositions of PGA, PBAT, PGA/PBAT (50/50) and the blending of between 10 and 30 wt.% AX8900. (b) FTIR showing the change in the OH peak in of PGA, PBAT, PGA/PBAT (50/50) and the blending of between 10 and 30 wt.% AX8900 and (c) FTIR showing the change in the ester peak in PGA, PBAT, PGA/PBAT (50/50) and the blending of between 10 and 30 wt.% AX8900.

The thermal stability of the PGA, PBAT, and the blends were investigated by TGA and shown in Figure 2. The $T_{5\%}$ onset degradation temperature for PBAT was 367.6 °C, while it was 299.5 °C for PGA. PGA/PBAT 50/50 blend had the $T_{5\%}$ onset degradation temperature at 311.6 °C, while the 50/50/10 blend showed a $T_{5\%}$ onset degradation temperature at 303.7 °C. The $T_{5\%}$ onset degradation temperature for the 50/50/20 blend and 50/50/30 blend were 306.4 °C and 315.7 °C, respectively. Evidently, from this, it can be established that all these functional blends were thermally stable up to 300 °C, well above the temperature used during to melt mix the blend components.

Figure 3(a) and (b) shows the 2nd heating and cooling curve from the DSC thermographs of PGA and its blends, respectively. Table 1 summarizes the associated key thermal transitions. For calculating % crystallinity (% X_c) of PGA in the blend, the following formula was used:

$$\% \ X_c = \frac{1}{w_f} \ \left(\frac{\Delta H_m}{\Delta H_f^0} \right) \ x \ 100 \tag{1}$$

where, w_f is the weight fraction of PGA in the blend, ΔH_m is the enthalpy of fusion of PGA derived from the second heating curve, and ΔH^o_f is the enthalpy of fusion of 100 % crystalline PGA (191.3 J/g).[19] Figure 3(a) shows that pristine PGA exhibited double melting peaks in the 2nd heating cycle, which are ascribed to the melting of primary crystals formed during isothermal crystallization of PGA and the subsequent melting of recrystallized crystals that formed during heating.[20] An increase in the melting temperature of PGA was observed in the blends containing AX8900 compared to the PGA/PBAT 50/50 blend. The effective blend T_g also increased with the incorporation of AX8900 in the blends. A similar slight shift in crystallization temperature was also observed in the cooling cycle of the blends, see Figure 3(b).

As shown in Table 1, while the pristine PGA had a %X_c of 45.1, with blending, it is dropped to 37.2 % for the PGA/PBAT 50/50 blend, whereas PBAT remained largely unaffected. After addition of 10 and 20 wt.% AX8900 (effective concentration in the final blend 9.1 wt.% and 16.68 wt.%, respectively), the % X_c of PGA increased to 45.6 and 48.0 %, respectively. This can be ascribed to the enhanced specific interactions between AX8900 and the polymer chains, dominated by hydrogen bonding. Comparatively, the %X_c of PBAT decreased to 5.5 and 8.9 %, respectively. The initial decrease in crystallinity was attributed to the reaction between AX8900 and PBAT. When the concentration was further increased to 30 wt.% (effective concentration in blend 23.06 wt.%), a drop in the *% X_c* of PGA was observed, whilst the %X_c increased further for PBAT indicating that the higher content of AX8900 was reacting with PBAT and compatibilizing PGA
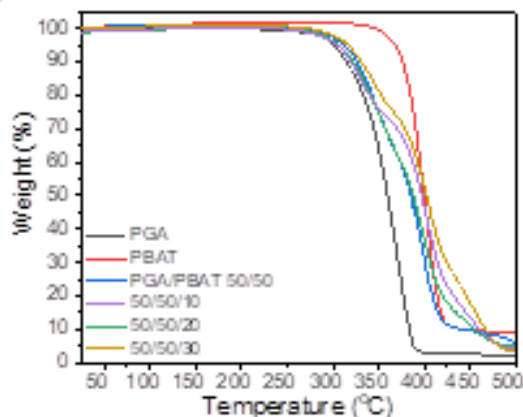

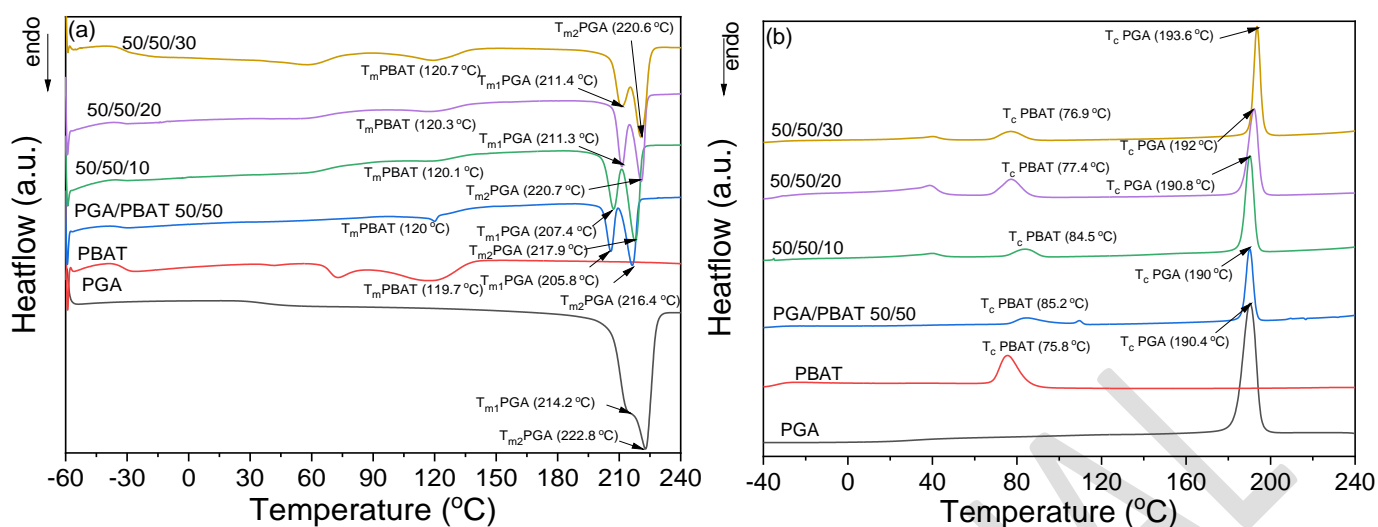**Figure 2**: TGA weight loss curves for PGA, PBAT and PGA/PBAT/AX8900 blends.

Figure 3: DSC thermographs of PGA, PBAT and their blends showing (a) 2nd heating curve, (b) cooling curve.

**Table 1:** DSC thermal transitions of the PGA and PBAT based blends.

Sample	T_g (°C) PBAT, PGA	T_m (°C) PGA	T_c (°C) PGA	T_m (°C) PBAT	T_c (°C) PBAT	$\% X_c$ PGA	$\% X_c$ PBAT
PGA	-, 51.4	214.2, 222.8	190.4	-	-	45.1	-
PBAT	-28.7, -	-	-	118.6	75.9	-	11.1
PGA/PBAT 50/50	-28.9, -	206.8, 217.5	190.5	120.6	83.9	37.2	13.4
50/50/10	-28.0, 37.9	207.4, 217.6	190.5	120.6	83.9	45.6	5.5
50/50/20	-30.19, 38.5	211.6, 220.5	194.0	119.8	77.1	48.0	8.9
50/50/30	-29.7, 39.4	211.1, 220.3	192.5	119.9	77.4	38.1	13.4

The effect of AX8900 on the mechanical properties of PGA/PBAT (50/50) is shown in Figure 4. While the average tensile stress of pristine PGA was 120 MPa and pristine PBAT was ~24 MPa, the uncompatibilized 50/50 blend had an average tensile stress of 7.5 MPa. PGA had an average strain at break of 5 % while that of PBAT was ~ 775 %. The uncompatibilized 50/50 blend exhibited an average

8

strain at break of 10.7 %, suggesting that the PGA and PBAT phases are not compatible. However, the tensile strength and the elongation at break of the PGA/PBAT blends improved with the addition of AX8900. There was a marginal increase in the tensile stress from 7.5 MPa to 10 MPa for 50/50/10 and to 10.5 MPa for 50/50/20 blends, respectively. Although, there was a significant enhancement in the elongation at break with addition of 10 % and 20 % AX8900, there was no improvement in the elongation at break after 20 % which suggests that AX8900 is an effective compatibilizer for the co-continuous PGA/PBAT blend only at concentrations <30 % (effective concentration 23.1 % by weight). PGA/PBAT/AX8900 50/50/20 showed the highest elongation at break of 145.2 ± 16.8 % and tensile stress compared to PGA/PBAT 50/50.

Figure 5 shows the difference in mechanical properties of the 50/50/20 AX8900 blends (tensile strength and strain at break) with values taken from the literature for other biodegradable co-continuous blends. Evidently it can be observed that in co-continuous regime, the blends exhibit low extension at break (<120 %). Further, pristine polymers like PGA, PLA and PLGA also exhibit low extension at break. But, with inclusion of AX8900 as a compatibilizer, the blends exhibited extension at break~ 150 % which is a key requirement for flexible packaging films.

Figure 6(a) and (b) shows the SEM micrographs taken of the fractured surfaces of PGA/PBAT 50/50 and PGA/PBAT/AX8900 50/50/20 blends. The cryo-fractured samples show that prior to introduction of AX8900, 50/50 PGA/PBAT blends show large phase separation with some spherical domains measuring over one hundred micrometers. Upon addition of 20 wt.% AX8900, the size of the phase separated domains decreased to between 20 μm – 100 μm and the number of phase separated domains also appeared reduced, indicating that AX8900 was compatibilising the two polymers together.
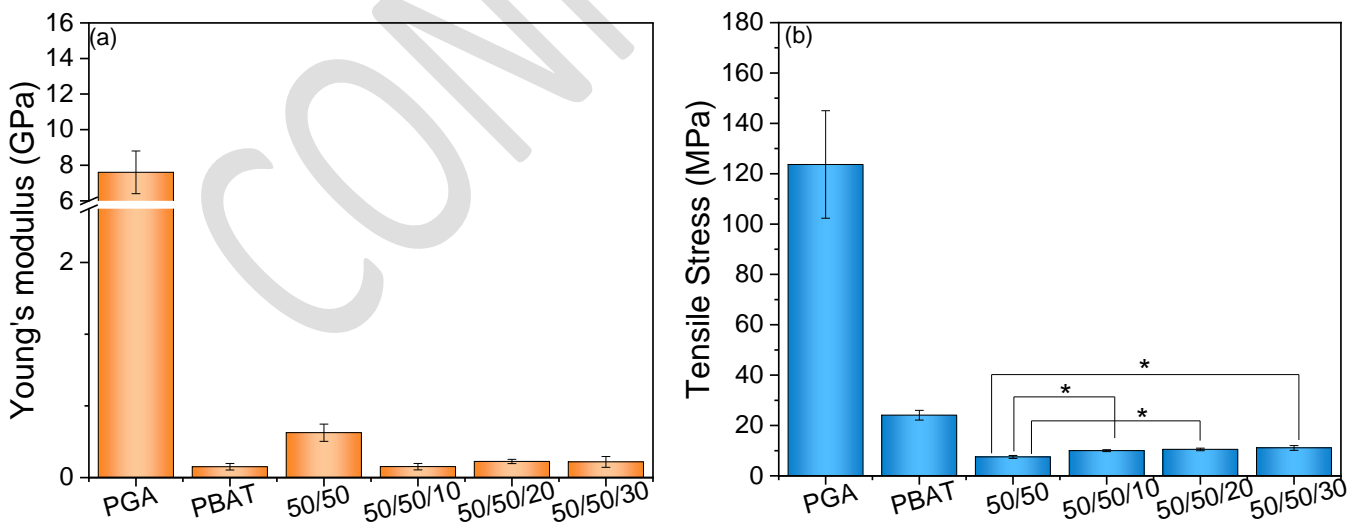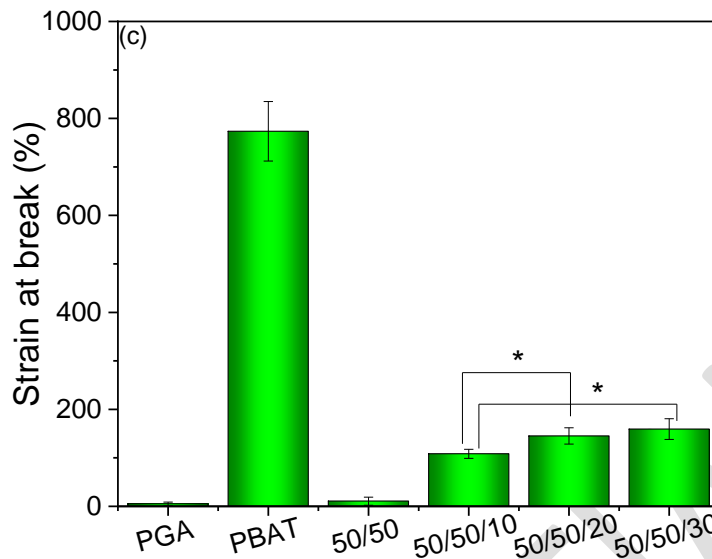
Figure 4: Effect of composition on the mechanical properties of PGA/PBAT blends. * indicates that the results are statistically significant. (Determined using ANOVA post-hoc analysis with p<0.05 and n=5 specimen.)
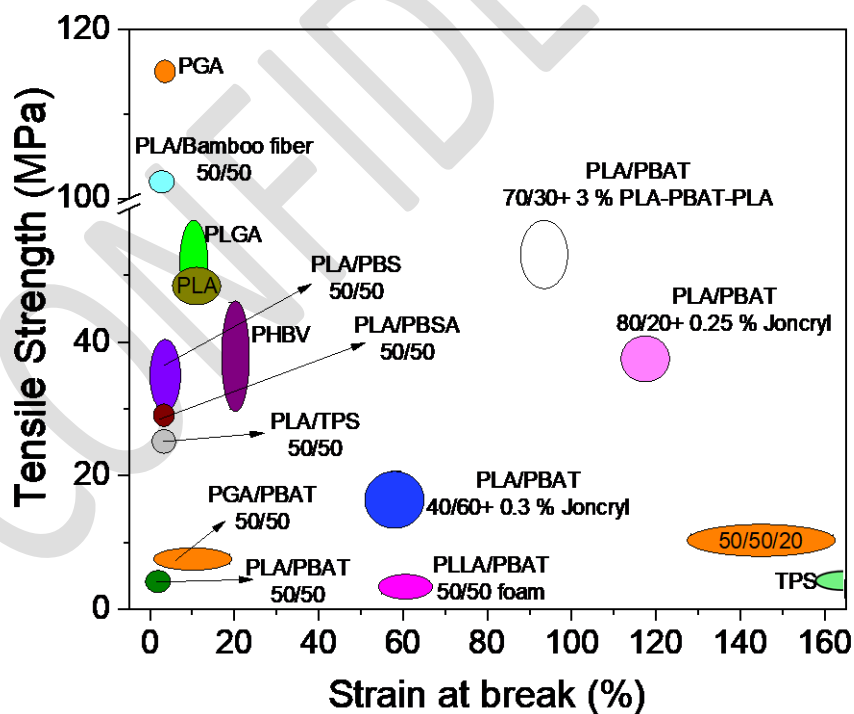

Figure 5: Tensile properties of biodegradable co-continuous blends from the literature. 70/30 and 80/20 blends of PLA/PBAT, pristine polymers are shown for comparison. The values plotted are taken from references [4, 21-30] Orange colour represents the results from this work.
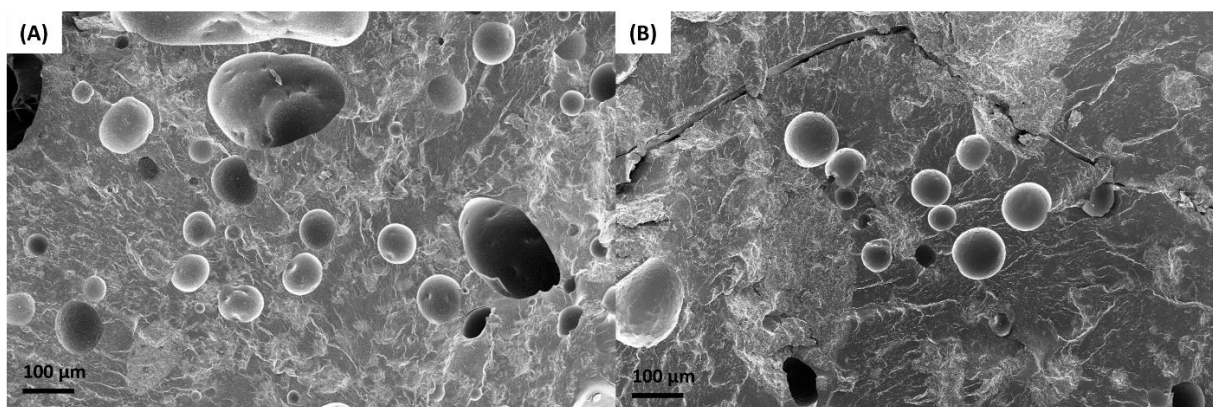
Figure 6: Surface SEM images of cryo-fractured a) PGA/PBAT 50/50 blend and b) PGA/PBAT/AX8900 50/50/20 blends.

Rheological characterisation of the polymer blends is shown in Figure 7. As 10wt.% compatibilizer is introduced, the storage modulus, loss modulus and complex viscosity of the polymer blend is unaffected across the entire frequency range examined. However, a small shift in the Cole-Cole plot, Figure 7c, shows a small increase in the storage modulus. This is due to interaction between 10 wt.% AX8900 operating *via* an interaction based compatibilising mechanism, but insufficiently compatibilising the PGA and PBAT. After introducing 20 wt.% AX8900, both the storage and loss modulus, and complex viscosity of PGA/PBAT (50/50) increased by one order of magnitude. In addition, the Cole-Cole plot shows a big increase in the storage modulus and confirms that AX8900 is compatibilising enough PGA and PBAT to significantly affect its physical properties. Finally, after the addition of 30 wt.% AX8900, a further increased of one order of magnitude is observed in the storage modulus and complex viscosity, but not the loss modulus, demonstrating an increase in the elastic behaviour of the blend. The greater increase in the storage modulus in the Cole-Cole plot shows that 30 wt.% AX8900 further increases the compatibility between PGA/PBAT, which is reflected in the mechanical properties of Figure 4. Furthermore, as the compatibiliser content is increased in PGA/PBAT (50/50), the crossover point for the liquid-to-solid like behaviour transition of the polymer blend occurs at higher frequencies, occurring at 0.05 Hz, 0.9 Hz and 27 Hz in 10 wt.% to 30 wt.% AX8900 additions, respectively. Without AX8900, this transition is not observed, see supporting Figure x, demonstrating the increased elastic behaviour of the blend.
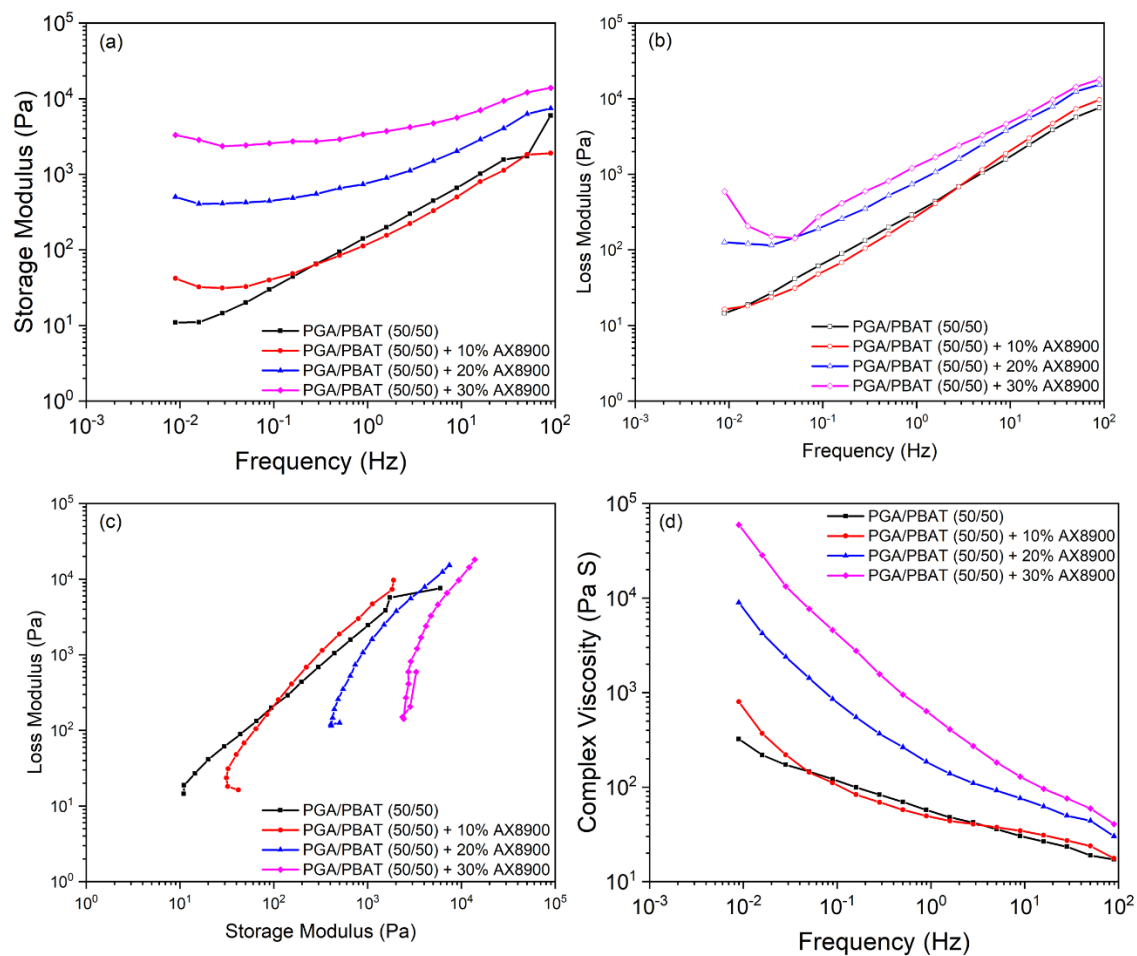
Figure 7: Rheology of PGA/PBAT (50/50) blends and addition of AX8900 compatibilizer up to 30% at 240 °C. (a) Storage modulus, (b) loss modulus, (c) Cole-Cole plot and (d) complex viscosity
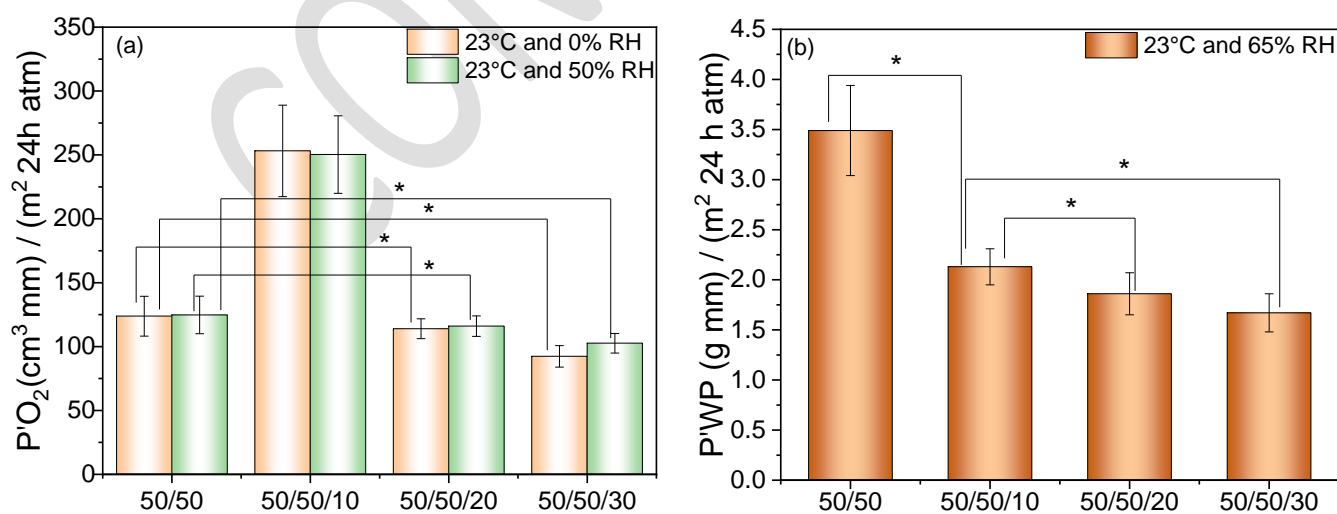

Figure 8: Oxygen and water vapour permeability data for AX8900 blends. (Statistical significance was determined ANOVA post-hoc analysis with $p < 0.05$ and $n = 3$ specimen per sample)

Figure 8(a) and (b) shows the permeability data of oxygen (P′O_2 at 23 °C and 0% RH and 50% RH) and water vapor (P′WV at 23 °C and 65% RH) for the polymers blends used in this study respectively. Kureha's PGA has an oxygen permeability of 0.013 cm^3 mm m^{-2} day^{-1} atm^{-1} at 20 °C and 80% RH[31] while from our study we observed the oxygen permeability of PBAT as 82.1 cm^3 mm m^{-2} day^{-1}atm^{-1} at 23°C and 50% RH. Since we have already established that PGA and PBAT were not compatible after blending, the av. oxygen permeability of 50/50 at 23°C and 50% RH was much higher than PBAT (P′O_2 = 124.73 cm^3 mm m^{-2} day^{-1}atm^{-1}). The oxygen permeability was even higher for the 50/50/10 blend, which can be plausibly explained by a double effect. On the one hand, the addition of 10 % AX8900 was not sufficient to induce enough compatibility between PGA and PBAT so to have a relevant effect on the diffusion of oxygen. On the other hand, the addition of AX8900 might have had a detrimental effect on the oxygen barrier performance to its mainly aliphatic chemical structure, that is, the hydrophobic tail suppresses the cohesion of the polymer network thus decreasing its density, which was eventually reflected in the dramatic increase of the oxygen permeability of the blend. With a AX8900 concentration > 20 %, the av. oxygen permeability value dropped significantly from 124.73 cm^3 mm m^{-2} day^{-1}atm^{-1} for 50/50 blend to 102.6 cm^3 mm m^{-2} day^{-1}atm^{-1} for 50/50/30 blends. In this case, the decrease in oxygen permeability can be explained considering the contribution of the increased amount of AX8900 to the compatibilization, which overcompensated the detrimental effect owing to the hydrophobic features of the AX8900 tail, as described before. This data supports the previous observations in mechanical properties as well. Apparently, the oxygen barrier performance was not improved upon increasing the amount of AX8900 up to 30 wt. %, corroborating the finding that after 20 wt. % of AX8900, any further addition of AX8900 in the polymer blend did not bring to any improvement.

The water vapour permeability of PGA was reported to be WP = 0.165 g mm m^2 day^{-1} atm^{-1} at 40 °C and 90% RH[31] while from our experiments, PBAT showed an av. water vapour permeability of 6.34 g mm m^2 day^{-1} atm^{-1} at 23°C and 65% RH. With blending a different scenario was observed. A decrease of ~ 40% in the av. water vapour permeability was seen for PGA/PBAT 50/50 blend. An additional improvement of the water vapour barrier performance was observed upon the addition of 10 wt. % and 20 wt. % AX8900 (~ 40% and ~ 47%, respectively, over the PGA/PBAT 50/50 sample). This trend, which was significantly different from what observed for the oxygen permeability, can be explained considering that AX8900 contributed to the improvement of the water vapour barrier performance both as a compatibilizer and by its hydrophobic tail, which acted as a chemical barrier to the diffusion of water molecules across the film thickness. However, as observed for the oxygen barrier performance, no statistically significant difference was observed in the P′WV value of the PGA/PBAT 50/50/30 sample, once again confirming that the most efficient concentration of AX8900 is 20 wt. %. We attempted to correlate the observations with crystallization behavior of PGA. However, we didn't see a direct trend between the barrier performance and crystallinity, probably due to the fact that facors

other than crystallinity affected the overall diffusion mechanism. For polymers like PLA, it is well established that polymorphism of crystals, the fraction of rigid amorphous content, and degree of space filling all contribute to the barrier performance.[32-34] We assume that since PGA is structurally similar to PLA, these important factors may also be valid for PGA as well and need further investigations.

Table 2 compares the permeability data obtained in our work with some commercial polymers and flexible films. It can be seen that although some polymers do exhibit lower oxygen and water vapour permeability but, due to improper waste segregation and plastic management practices, they contribute to plastics pollution. PGA and PBAT both are completely biodegradable and can close the plastics recycling loop. Further, the barrier properties are comparable to the conventional polymers making them suitable for packaging applications

Table 2: Comparison of oxygen and water vapour permeability of commercial polymer films with the present work. The values are from reference [35]

Polymers	P′O$_2$ (cm³·mm/m²·day·atm)	P′WV (g·mm/m²·day)
BASF Terluran ABS Film	45.6 – 81	3.1
Dow Acrylonitrile ABS Films	47 – 102	2.0 - 6.3
Dow Trycite Oriented PS Film	98 – 138	1.3
BASF AG Polystyrol 168 N GPPS Film	101	1.2
High Density Polyethylene (HDPE)	26.3 - 98.5	0.1 - 0.24
Mid Density Polyethylene (MDPE)	98.5 – 210	0.4 - 0.6
Low Density Polyethylene (LDPE)	98 – 453	0.39 - 0.59
DuPont Mylar Films Polyethylene Naphthalate (PEN)	1.13 - 1.18	0.38 - 0.57
Fluorinated ethylene propylene (FEP)	295 – 394	0.087
Polytetrafluoroethylene (PTFE)	222 – 387	0.0045 - 0.30
Ethylene Vinyl Alcohol (EVOH)	0.01 - 0.15	0.8 - 2.4
Polyvinylidene Chloride (PVDC)	0.00425 - 0.57	0.025 - 0.913
DOW Saran PVDC Films	0.00425 - 0.00625	
PGA (this work)	46.61 - 61.21*	4.78 - 5.68**
PBAT (this work)	71.4 - 92.8*	5.58 - 7.1**
PGA/PBAT 50/50 (this work)	110.03 - 139.43*	3.04 - 3.94**
PGA/PBAT/AX8900 50/50/20 (this work)	104.01 - 128.01*	1.65 – 2.07**

* At 23°C and 50% RH, ** At 23°C and 65% RH

Conclusions

In the present work, we investigated the compatibilization of co-continuous biodegradable polymer blends of PGA and PBAT by using a unique epoxy-based compatibilizer Lotader AX8900. The blends were characterized using DSC, TGA, and FTIR, while mechanical properties were evaluated using UTM. It was observed that the compatibilized blends exhibited good thermal stability up to 300 $^{\circ}$C, and the 50/50/20 blend was the best among all compositions. This blend exhibited good extension at a break of 145.21 $\pm$ 16.82 % and had a spherical morphology as observed after the cryofracture of the samples. Rheological analysis showed that the introduction of the compatibilizer increased the elastic behaviour of the blend as the PBAT and PGA were compatibilized. It was observed that 20 wt.% AX8900 was required to have a significant effect on the physical properties of the polymer blend. The blend also exhibited a superior barrier to oxygen and water vapour with oxygen permeability and water vapour permeation 116.01 $\pm$ 12.0 cm³·mm/m²·day·atm and 1.86 $\pm$ 0.21g·mm/m²·day respectively. Taken together, the proposed biodegradable blend may be suitable for thermally stable packaging applications.

Conflicts of interest

There are no conflicts to declare.

Acknowledgments

References:

1. Razza, F.; Innocenti, F. D., Bioplastics from renewable resources: the benefits of biodegradability. *Asia-Pacific Journal of Chemical Engineering* **2012,** *7*, S301-S309.
2. Lackner, M., Bioplastics. *Kirk-Othmer Encyclopedia of Chemical Technology* **2000**, 1-41.
3. *Bioplastics Market Development Update*; European Bioplastics: Berlin, Germany, **2019**.
4. Samantaray, P. K.; Little, A.; Haddleton, D. M.; McNally, T.; Tan, B.; Sun, Z.; Huang, W.; Ji, Y.; Wan, C., Poly(glycolic acid) (PGA): a versatile building block expanding high performance and sustainable bioplastic applications. *Green Chemistry* **2020,** *22* (13), 4055-4081.
5. K. Jim Jem, B. T., The Development and Challenges of Poly (lactic acid) and Poly (glycolic acid). *Advanced Industrial and Engineering Polymer Research* **2020**.
6. Moustafa, H.; El Kissi, N.; Abou-Kandil, A. I.; Abdel-Aziz, M. S.; Dufresne, A., PLA/PBAT Bionanocomposites with Antimicrobial Natural Rosin for Green Packaging. *ACS Appl Mater Interfaces* **2017,** *9* (23), 20132-20141.
7. Witt, U.; Einig, T.; Yamamoto, M.; Kleeberg, I.; Deckwer, W. D.; Muller, R. J., Biodegradation of aliphatic-aromatic copolyesters: evaluation of the final biodegradability and ecotoxicological impact of degradation intermediates. *Chemosphere* **2001,** *44* (2), 289-99.

8.   Jiang, L.; Wolcott, M. P.; Zhang, J., Study of biodegradable polylactide/poly (butylene adipate-co-terephthalate) blends. *Biomacromolecules* **2006,** *7* (1), 199-207.

9.   Dong, W.; Zou, B.; Yan, Y.; Ma, P.; Chen, M., Effect of Chain-Extenders on the Properties and Hydrolytic Degradation Behavior of the Poly (lactide)/Poly (butylene adipate-co-terephthalate) Blends. *International journal of molecular sciences* **2013,** *14* (10), 20189-20203.

10.   Han, Y.; Shi, J.; Mao, L.; Wang, Z.; Zhang, L., Improvement of Compatibility and Mechanical Performances of PLA/PBAT Composites with Epoxidized Soybean Oil as Compatibilizer. *Industrial & Engineering Chemistry Research* **2020**.

11.   Correa-Pacheco, Z. N.; Black-Solís, J. D.; Ortega-Gudiño, P.; Sabino-Gutiérrez, M. A.; Benítez-Jiménez, J. J.; Barajas-Cervantes, A.; Bautista-Baños, S.; Hurtado-Colmenares, L. B., Preparation and characterization of bio-based PLA/PBAT and cinnamon essential oil polymer fibers and life-cycle assessment from hydrolytic degradation. *Polymers* **2020,** *12* (1), 38.

12.   Ma, P.; Cai, X.; Zhang, Y.; Wang, S.; Dong, W.; Chen, M.; Lemstra, P. J., In-situ compatibilization of poly(lactic acid) and poly(butylene adipate-co-terephthalate) blends by using dicumyl peroxide as a free-radical initiator. *Polymer Degradation and Stability* **2014,** *102*, 145-151.

13.   Dong, W.; Zou, B.; Ma, P.; Liu, W.; Zhou, X.; Shi, D.; Ni, Z.; Chen, M., Influence of phthalic anhydride and bioxazoline on the mechanical and morphological properties of biodegradable poly(lactic acid)/poly[(butylene adipate)-co-terephthalate] blends. *Polymer International* **2013,** *62* (12), 1783-1790.

14.   Lin, S.; Guo, W.; Chen, C.; Ma, J.; Wang, B., Mechanical properties and morphology of biodegradable poly(lactic acid)/poly(butylene adipate-co-terephthalate) blends compatibilized by transesterification. *Materials & Design (1980-2015)* **2012,** *36*, 604-608.

15.   Sarul, D. S.; Arslan, D.; Vatansever, E.; Kahraman, Y.; Durmus, A.; Salehiyan, R.; Nofar, M., Preparation and characterization of PLA/PBAT/CNC blend nanocomposites. *Colloid and Polymer Science* **2021**, 1-12.

16.   da Silva, J. M. F.; Soares, B. G., Epoxidized cardanol-based prepolymer as promising biobased compatibilizing agent for PLA/PBAT blends. *Polymer Testing* **2021,** *93*, 106889.

17.   Abdelwahab, M. A.; Jacob, S.; Misra, M.; Mohanty, A. K., Super-tough sustainable biobased composites from polylactide bioplastic and lignin for bio-elastomer application. *Polymer* **2021,** *212*, 123153.

18.   Shechter, L.; Wynstra, J., Glycidyl ether reactions with alcohols, phenols, carboxylic acids, and acid anhydrides. *Industrial & Engineering Chemistry* **1956,** *48* (1), 86-93.

19.   Chu, C., Differential scanning calorimetric study of the crystallization kinetics of polyglycolic acid at high undercooling. *Polymer* **1980,** *21* (12), 1480-1482.

20.   Yu, C.; Bao, J.; Xie, Q.; Shan, G.; Bao, Y.; Pan, P., Crystallization behavior and crystalline structural changes of poly (glycolic acid) investigated via temperature-variable WAXD and FTIR analysis. *CrystEngComm* **2016,** *18* (40), 7894-7902.

21.   Homklin, R.; Hongsriphan, N., Mechanical and thermal properties of PLA/PBS co-continuous blends adding nucleating agent. *Energy Procedia* **2013,** *34*, 871-879.

22.   Barbosa, J. D. V.; Azevedo, J. B.; Araújo, E. M.; Machado, B. A. S.; Hodel, K. V. S.; Mélo, T. J. A. d., Bionanocomposites of PLA/PBAT/organophilic clay: preparation and characterization. *Polímeros* **2019,** *29* (3).

23.   Kang, Y.; Chen, P.; Shi, X.; Zhang, G.; Wang, C., Preparation of open-porous stereocomplex PLA/PBAT scaffolds and correlation between their morphology, mechanical behavior, and cell compatibility. *RSC advances* **2018,** *8* (23), 12933-12943.

24.   Nofar, M.; Salehiyan, R.; Ciftci, U.; Jalali, A.; Durmuş, A., Ductility improvements of PLA-based binary and ternary blends with controlled morphology using PBAT, PBSA, and nanoclay. *Composites Part B: Engineering* **2020,** *182*, 107661.

25.   Arruda, L. C.; Magaton, M.; Bretas, R. E. S.; Ueki, M. M., Influence of chain extender on mechanical, thermal and morphological properties of blown films of PLA/PBAT blends. *Polymer Testing* **2015,** *43*, 27-37.

26.   Ding, Y.; Lu, B.; Wang, P.; Wang, G.; Ji, J., PLA-PBAT-PLA tri-block copolymers: Effective compatibilizers for promotion of the mechanical and rheological properties of PLA/PBAT blends. *Polymer Degradation and Stability* **2018,** *147*, 41-48.

27.   Al-Itry, R.; Lamnawar, K.; Maazouz, A., Improvement of thermal stability, rheological and mechanical properties of PLA, PBAT and their blends by reactive extrusion with functionalized epoxy. *Polymer Degradation and Stability* **2012,** *97* (10), 1898-1914.

28.   Okubo, K.; Fujii, T.; Yamashita, N., Improvement of interfacial adhesion in bamboo polymer composite enhanced with micro-fibrillated cellulose. *JSME International Journal Series A Solid Mechanics and Material Engineering* **2005,** *48* (4), 199-204.

29.   Mittal, V.; Akhtar, T.; Matsko, N., Mechanical, thermal, rheological and morphological properties of binary and ternary blends of PLA, TPS and PCL. *Macromolecular Materials and Engineering* **2015,** *300* (4), 423-435.

30.   Li, G.; Favis, B. D., Morphology Development and Interfacial Interactions in Polycaprolactone/Thermoplastic-Starch Blends. *Macromolecular Chemistry and Physics* **2010,** *211* (3), 321-333.

31.   Murcia Valderrama, M. A.; van Putten, R. J.; Gruter, G. M., PLGA Barrier Materials from CO2. The influence of Lactide Co-monomer on Glycolic Acid Polyesters. *ACS Appl Polym Mater* **2020,** *2* (7), 2706-2718.

32.   Guinault, A.; Sollogoub, C.; Ducruet, V.; Domenek, S., Impact of crystallinity of poly (lactide) on helium and oxygen barrier properties. *European Polymer Journal* **2012,** *48* (4), 779-788.

33.   Cocca, M.; Di Lorenzo, M. L.; Malinconico, M.; Frezza, V., Influence of crystal polymorphism on mechanical and barrier properties of poly (l-lactic acid). *European Polymer Journal* **2011,** *47* (5), 1073-1080.

34.   Drieskens, M.; Peeters, R.; Mullens, J.; Franco, D.; Lemstra, P. J.; Hristova-Bogaerds, D. G., Structure versus properties relationship of poly (lactic acid). I. Effect of crystallinity on barrier properties. *Journal of Polymer Science Part B: Polymer Physics* **2009,** *47* (22), 2247-2258.

35.   Abbott, S. Permeability Calculations. https://www.stevenabbott.co.uk/practical-coatings/permeability.php (accessed 28 January).